Adsorption Mechanism and Uptake of Methane in Covalent Organic Frameworks: Theory and Experiment

José L. Mendoza-Cortés,[†] Sang Soo Han,[†,‡] Hiroyasu Furukawa,[§] Omar M. Yaghi,*,[§] and William A. Goddard III*,[†]

Materials and Process Simulation Center, California Institute of Technology, Pasadena, California 91106, and Center for Reticular Chemistry, Department of Chemistry and Biochemistry, University of California, Los Angeles, California 90095

We determined the methane (CH_4) uptake (at 298 K and 1 to 100 bar pressure) for a variety of covalent organic frameworks (COFs), including both two-dimensional (COF-1, COF-5, COF-6, COF-8, and COF-10) and three-dimensional (COF-102, COF-103, COF-105, and COF-108) systems. For all COFs, the CH_4 uptake was predicted from grand canonical Monte Carlo (GCMC) simulations based on force fields (FF) developed to fit accurate quantum mechanics (QM) [second order Møller−Plesset (MP2) perturbation theory using doubly polarized quadruple-ζ (QZVPP) basis sets]. This FF was validated by comparison with the equation of state for CH_4 and by comparison with the experimental uptake isotherms at 298 K (reported here for COF-5 and COF-8), which agrees well (within 2% for 1−100 bar) with the GCMC simulations. From our simulations we have been able to observe, for the first time, multilayer formation coexisting with a pore filling mechanism. The best COF in terms of total volume of CH_4 per unit volume COF absorbent is COF-1, which can store 195 v/v at 298 K and 30 bar, exceeding the U.S. Department of Energy target for CH_4 storage of 180 v/v at 298 K and 35 bar. The best COFs on a delivery amount basis (volume adsorbed from 5 to 100 bar) are COF-102 and COF-103 with values of 230 and 234 v(STP: 298 K, 1.01 bar)/v, respectively, making these promising materials for practical methane storage.

1. Introduction

Although gasoline is the current fuel of choice for personal transportation because of its low-cost and the fuel supply structure, it generates pollutants by combustion and evaporation, including nitrogen oxides, sulfur oxide, carbon monoxide, and traces of carcinogens chemicals.[1] This has motivated the search for alternative routes toward new energy sources. Methane is a good candidate for an alternative fuel because it is inexpensive with clean-burning characteristics.[2] Moreover, the huge reserves of natural gas (NG) (>95% CH_4, with some ethane, nitrogen, higher hydrocarbons, and carbon dioxide)[2] around the world are comparable to the energy content of the world's petroleum reserves. However, to utilize this CH_4, inexpensive means of transporting and storing are required. Since methane has a critical temperature of 191 K and critical pressure of 46.6 bar, it cannot be liquefied at room temperature, increasing the cost of its transportation.[3] Attempts to overcome this disadvantage include

• storing methane as liquefied natural gas (LNG, at ∼112 K) or compressed natural gas (CNG, at ∼200 bar),[4]

• converting methane to oxygenates such as methanol or higher hydrocarbons such as ethane,[5−7] and

• storing in porous materials.[8]

Among these alternatives, we believe that storing methane via adsorption on porous materials is the most promising near-term route because it allows operation at reasonable pressure (1−300 bar) and temperature (7−298 K) and does not require extra energy input for conversion to higher hydrocarbons or methanol.
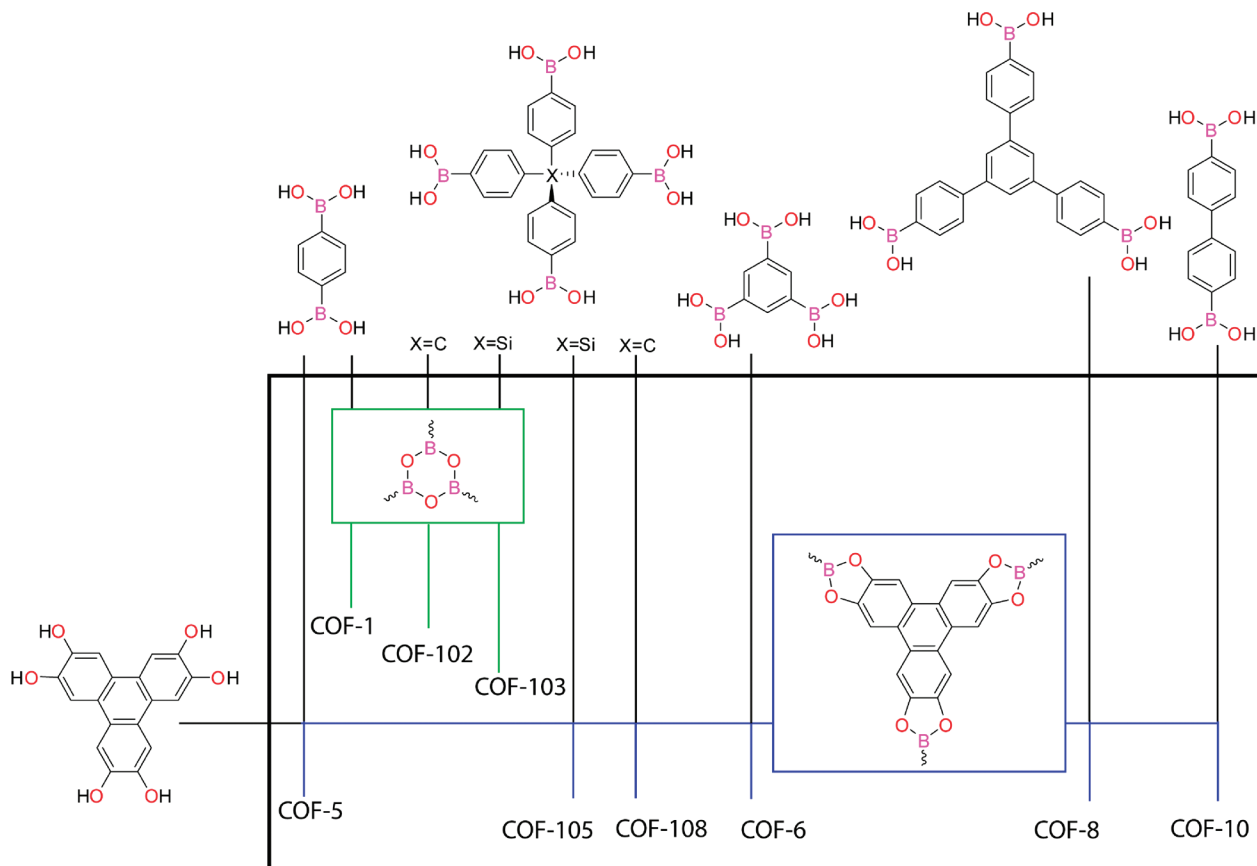
Recently, the new covalent-organic frameworks (COFs) family of porous materials was reported, based on boronic acid building blocks (Figure 1).[9−12] COFs are held together by strong covalent bonds between light elements such as B, C, O, H, and Si. They have high surface areas (as high as 6450 m^2/g), large pore volumes (as high as 5.4 cm^3/g), and the lowest densities for any known crystalline material (as low as 0.17 g/cm^3),[11] all of which are prerequisites for high uptake of methane (Table 1). In principle, an immense number of COFs using various building units and various numbers of points of extension and functionality to attain various topologies could be synthesized and tested for methane adsorption. Such empirical processes have been effective, but we explore here the alternate procedure in which theory and computation is used to predict the most promising candidates, followed by experimental synthesis and characterization only on the most promising cases. Of course, this is only possible if the results from the theory and computation are sufficiently reliable that one can with confidence reject low performance systems without the need for experiment. Grand canonical Monte Carlo (GCMC) provides the accuracy required to predict accurate adsorption isotherms. However, GCMC requires a force field (FF) accurate for predicting the structure of the COF and for predicting the weak intermolecular interactions with CH_4. The covalent bonds of the framework for COF systems are well treated by generic FF such as Dreiding[13] and UFF,[14] and by more specialized FF such as OPLS.[15] However, these FF do not generally provide the accuracy required to predict adsorption isotherms.[16] GCMC

_____

* Corresponding authors. E-mail: O.M.Y., yaghi@chem.ucla.edu; W.A.G., wag@wag.caltech.edu. Phone: O.M.Y., 310-206-0398; W.A.G., 626-395-2731. Fax: O.M.Y., 310-206-5891; W.A.G., 626-585-0918.
　† California Institute of Technology.
　‡ Present address: Korea Research Institute of Standards and Science, Daejeon, 305-340, Republic of Korea.
　§ University of California.

Methane in Covalent Organic Frameworks

J. Phys. Chem. A, Vol. 114, No. 40, 2010 **10825**

Figure 1. Molecular structures of building units used for COF synthesis (outside black box) and their COF formation reactions (green box, boroxine; blue box, ester).

TABLE 1: Pore Size (P_{Size}), Surface Area (S_A), Pore Volume (V_P), and Density of the Framework without Guest Molecules (ρ) for the Studied COF Series[a]

material	P_{Size}, Å	S_A, m² g⁻¹	V_P, cm³ g⁻¹	ρ, g cm⁻³	topology	space group
COF-1	7	1230	0.38	0.91	gra	$P6_3/mmc$
COF-5	27	1520	1.17	0.58	bnn	$P6/mmm$
COF-6	11	1050	0.55	1.03	bnn	$P6/mmm$
COF-8	16	1320	0.87	0.71	bnn	$P6/mmm$
COF-10	35	1830	1.65	0.49	bnn	$P6/mmm$
COF-102	12	4940	1.81	0.42	ctn	$I\bar{4}3d$
COF-103	12	5230	2.05	0.38	ctn	$I\bar{4}3d$
COF-105	19	6450	4.94	0.18	ctn	$I\bar{4}3d$
COF-108	20, 11	6280	5.40	0.17	ctn	$P\bar{4}3m$

[a] P_{Size} was calculated by placing a sphere in the center of the largest cavity and measuring its diameter considering the van der Waals radii of atoms in the framework. S_A and V_p were estimated from rolling an Ar molecule with diameter of 3.42 Å[33] over the framework's surface.
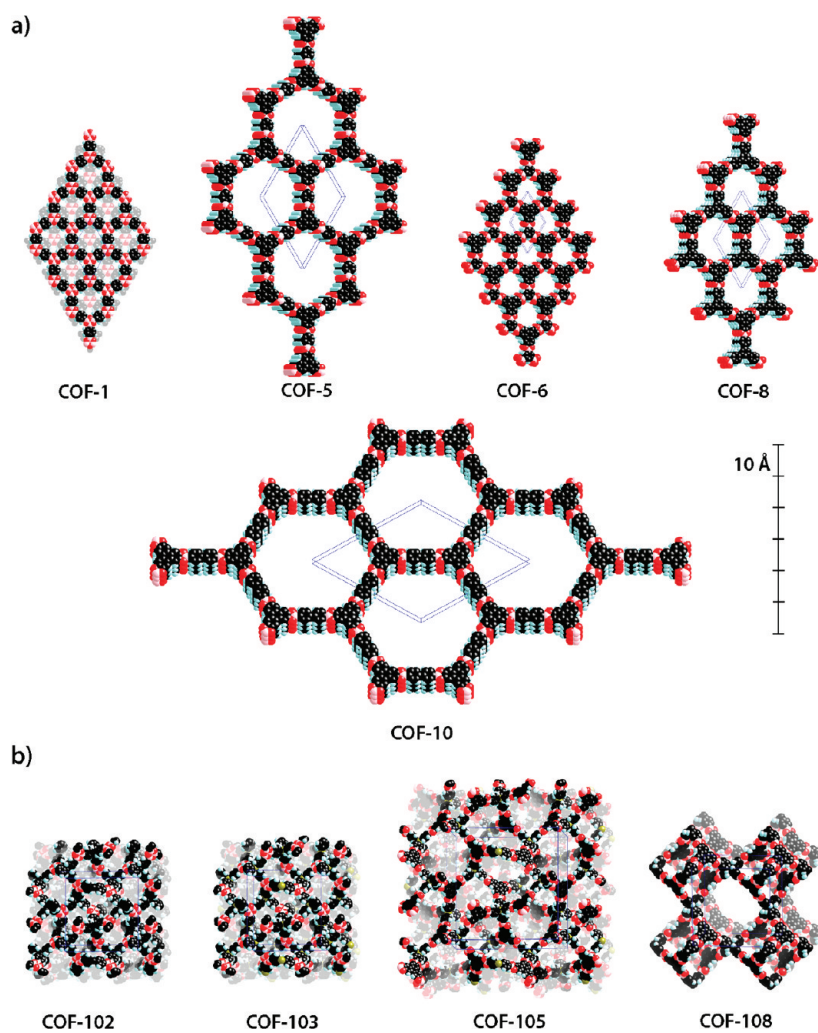
coupled to these generic FF have been used to reproduce experimental isotherms reported by our group in some 2D-COFs[17] and 3D-COFs[18] finding disagreements between our experiments and this theory of 10% and 25%, respectively. The same approach has been used to study MOF-5, and they were compared to experiments and the absolute error ranges from +5 to −16%.[19−21] Here it is essential to account for the van der Waals (vdW) attraction (London dispersion) and electrostatic interactions that dominate the interaction of CH_4 with surfaces. The vdW terms have been a problem because the powerful density-functional theory (DFT) methods underlying most quantum mechanics (QM) calculations today are notoriously inaccurate for vdW.[22,23] Consequently, we focused here on developing and validating the vdW part of the force field using QM methods (MP2) expected to be accurate.

In this work, we predict the methane uptake for five 2D-COFs (COF-1, COF-5, COF-6, COF-8, and COF-10) and four 3D-COFs (COF-102, COF-103, COF-105, and COF-108), as shown in Figure 2. However, a better adjective for 2D- is two-periodic-COFs and for 3D- is three-periodic-COFs. These predicted isotherms are in excellent agreement with our experimental results (within 2%) for the two systems for which the experimental data show that the pores of the structures have been completely cleaned (COF-5 and COF-8 up to 85 bar), validating our computational methodology. Then we use this method to show that COF-102 and 103 are excellent materials for practical methane storage.

2. Methodology

2.1. Force Field. For geometry optimization, we used the quadruple-ζ valence basis (QZV) supplemented with polarization functions from the cc-pVTZ basis, which is denoted as QZVPP. To develop the FF to be used in describing the interactions of methane with the COF (CH_4−COF) and the interaction between methane molecules (CH_4−CH_4), we used QM at the MP2 level with the approximate resolution of the identity (RI-MP2).[24−26] Quantum mechanical calculations were performed using the Turbomole code. The auxiliary-QZVPP basis set was used for the RI-MP2 calculations.[27] We did not include excitations out of the 1s core orbital in the MP2 calculation.

The binding energies between CH_4−CH_4 and CH_4−COFs were corrected using basis-set superposition error (BSSE) by the full counterpoise procedure (eq 1).

a)

COF-1   COF-5   COF-6   COF-8

10 Å

COF-10

b)

COF-102   COF-103   COF-105   COF-108

Figure 2. Atomic connectivity and structure of crystalline products for (a) 2D-COFs and (b) 3D- COFs. Unit cells are shown in blue lines. Atoms colors: C, black; O, red; B, pink; Si, yellow; H, blue.

$$E_{\text{interaction}}^{\text{CP}} = E_{\text{super}} - \sum_{i=1}^{n} E_{m_{\text{opt}}^i} + \sum_{i=1}^{n} (E_{m_{\text{f}}^i} - E_{m_{\text{f}}^{i*}}) \quad (1)$$

Here the E_m^s represents the energies of the individual monomers. The subscripts opt and f denote the individually optimized monomers and those frozen in their super molecular geometries, respectively. The asterisk (*) denotes monomers calculated with ghost orbitals.[28]

Using the accurate RI-MP2 results, we developed FF parameters for nonbonded interactions between CH_4-CH_4 and CH_4-COFs where for the functional form the Morse potential (eq 2) was used. Here the parameter D is the well depth, r_0 is the equilibrium bond distance, and α determines the stiffness (force constant).

$$\mathbf{U}_{ij}^{\text{Morse}}(r_{ij}) = D\{e^{\alpha(1-r_{ij}/r_0)} - 2e^{\alpha/2(1-r_{ij}/r_0)}\} \quad (2)$$

It is more common to use Lennard-Jones (LJ-12-6) and exponential-6 (exp-6) functional forms for such studies,[13] because it is believed that the long-range form should have $1/R^6$ character. However, our experience is that LJ-12-6 and exp-6 have inner walls that are too stiff and that the region of true $1/R^6$ character is only at much longer distances than relevant here. Thus, we believe that the Morse function is the most suitable for studying gas adsorption in porous frameworks. For
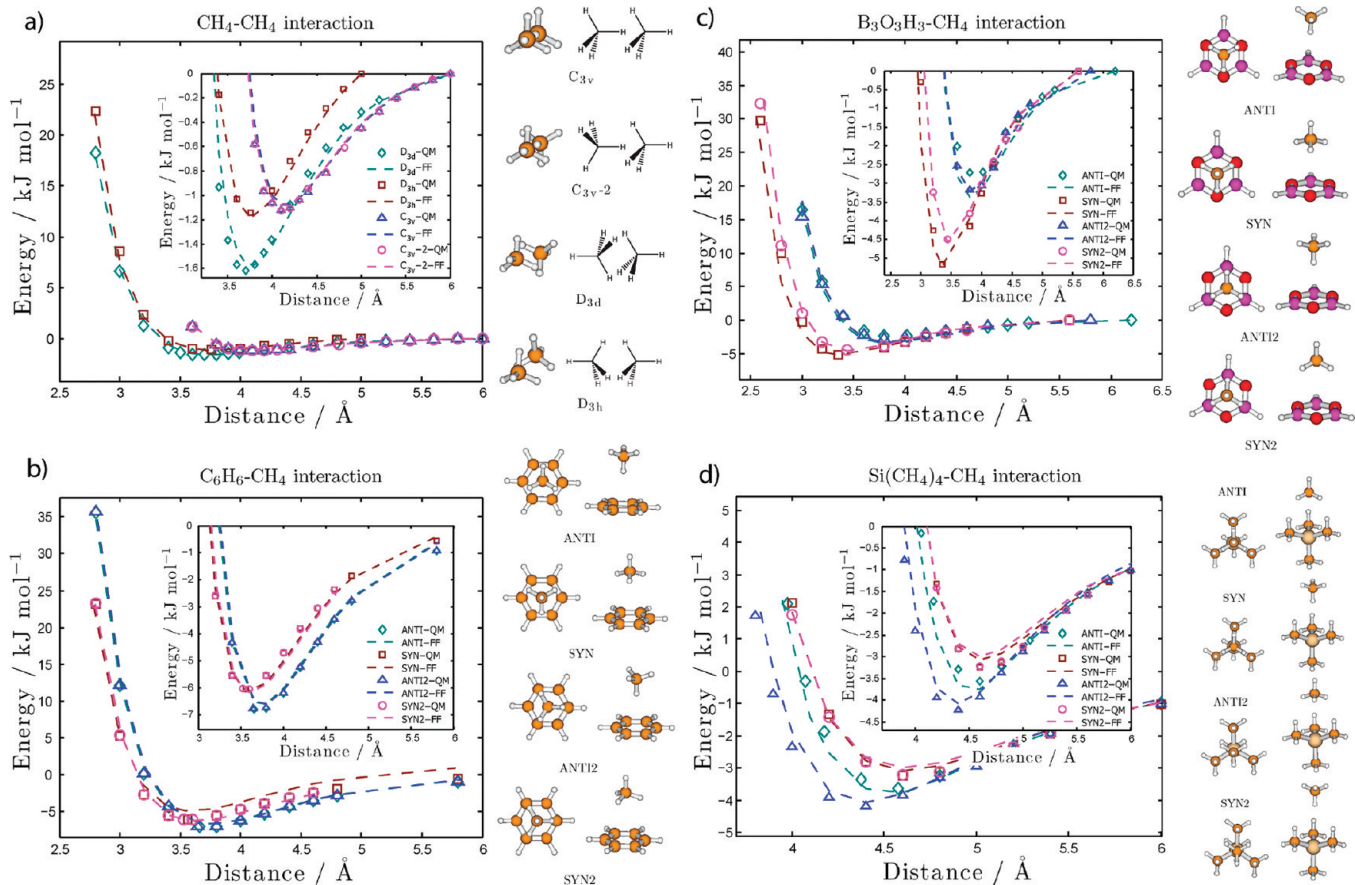
the electrostatic interactions, we used the atomic charges (C −0.43820 and H +0.10955) of methane from our QM calculations. For the charges of the COFs framework we used the QEq charge equilibration method.[29]

2.2. QM Determination of the vdW Force Field Parameters. The parameters (D, α, and r_0 in eq 2) were developed to fit QM results. Since all COF systems considered here are composed only of B, C, H, O, and Si, we developed 13 sets of interaction parameters:

- $C_{CH_4}-C_{CH_4}$, $H_{CH_4}-H_{CH_4}$, $C_{CH_4}-H_{CH_4}$
- $C_{COF}-C_{CH_4}$, $C_{COF}-H_{CH_4}$, $H_{COF}-C_{CH_4}$, $H_{COF}-H_{CH_4}$
- $O_{COF}-C_{CH_4}$, $O_{COF}-H_{CH_4}$, $B_{COF}-C_{CH_4}$, $B_{COF}-H_{CH_4}$
- $Si_{COF}-C_{CH_4}$, $Si_{COF}-H_{CH_4}$

To obtain these parameters, we considered four different geometrical configurations for each cluster: CH_4-CH_4, $C_6H_6-CH_4$, $B_3O_3H_3-CH_4$, and $Si(CH_4)_4-CH_4$ (Figure 3) as well as the interaction with the edges.[30]

Our RI-MP2/QZVPP calculation finds that the energy for CH_4 binding (E_{bind}) to the face of the organic linker for the most stable configuration is higher than when it interacts with the edge; also the equilibrium distance (R_{eq}) to the face is shorter. The face E_{bind} of $CH_4-C_6H_6$ is 7.0 kJ mol^{-1} with R_{eq} equal to 3.7 Å, while the edge E_{bind} is 3.8 kJ mol^{-1} and R_{eq} is 5.0 Å. Also, the face E_{bind} for $CH_4-B_3O_3H_3$ is 5.2 kJ mol^{-1} and R_{eq} is 3.4 Å, whereas its edge E_{bind} is 1.5 kJ mol^{-1} and R_{eq} is 4.9 Å.

Methane in Covalent Organic Frameworks

J. Phys. Chem. A, Vol. 114, No. 40, 2010 **10827**

Figure 3. Comparison of the optimized FF energies with QM (MP2-RI) for four configurations: (a) CH_4-CH_4; (b) $C_6H_6-CH_4$; (c) $B_3O_3H_3-CH_4$; (d) $Si(CH_4)_4-CH_4$. FF results are shown as dashed lines while the QM results are shown by empty symbols. Each configuration has four plausible geometrical structures shown to the right where C atoms are brown, B pink, O red, Si yellow, and H white. Configurations interacting through the edges are not shown. The insets show the accuracy in fitting to the equilibrium distance. Data plotted here as the BSSE corrections are included in the Supporting Information.

TABLE 2: Nonbonded FF Parameters Developed To Fit the RI-MP2 Calculations[a]

term	D/kJ mol^{-1}	r_0/Å	α
$C_{CH4}-C_{CH4}$	3.21×10^{-1}	3.92	12.7
$H_{CH4}-H_{CH4}$	1.34×10^{-2}	3.13	11.4
$C_{CH4}-H_{CH4}$	2.18×10^{-1}	3.46	11.0
$C_{COF}-C_{CH4}$	2.09×10^{-1}	4.23	13.2
$H_{COF}-C_{CH4}$	3.67×10^{-3}	3.25	12.0
$O_{COF}-C_{CH4}$	2.02×10^{-1}	3.59	11.3
$B_{COF}-C_{CH4}$	1.95×10^{-1}	4.11	12.3
$C_{COF}-H_{CH4}$	4.79×10^{-1}	3.08	9.07
$H_{COF}-H_{CH4}$	3.67×10^{-3}	3.26	12.0
$O_{COF}-H_{CH4}$	3.85×10^{-1}	2.55	8.99
$B_{COF}-H_{CH4}$	3.84×10^{-1}	3.28	11.7
$Si_{COF}-H_{CH4}$	4.58×10^{-1}	4.06	7.19
$Si_{COF}-C_{CH4}$	3.58×10^{-1}	4.78	16.5

[a] The function form (Morse) is given in eq 2. D is the well depth, r_0 is the equilibrium bond distance, and α determines the force constant. Each parameter has been rounded to three significant figures.

The energy as a function of distance from QM was calculated near the equilibration distance for each type of interaction and fitted to eq 2 using larger weights at the equilibrium distances (insets in Figure 3). The predominant configurations interactions for the clusters are D_{3d} for CH_4-CH_4, ANTI for $C_6H_6-CH_4$, SYN for $B_3O_3H_3-CH_4$, and ANTI2 for $Si(CH_4)_4-CH_4$. Our new FF parameters (Table 2) reproduce well these binding energies and the QM energy profile (Table 3). We validated the FF for CH_4 by calculating the CH_4 equation of state at various

TABLE 3: Most Stable Interaction Geometries for Clusters Considered in This Work[a]

interaction	geometry	r_0/Å	QM/kJ mol^{-1}	FF/kJ mol^{-1}
CH_4-CH_4	D_{3d}	3.710	1.61	1.59
$C_6H_6-CH_4$	ANTI	3.657	7.01	6.83
$B_3O_3H_3-CH_4$	SYN	3.352	5.16	5.22
$Si(CH_4)_4-CH_4$	ANTI2	4.401	4.44	4.28
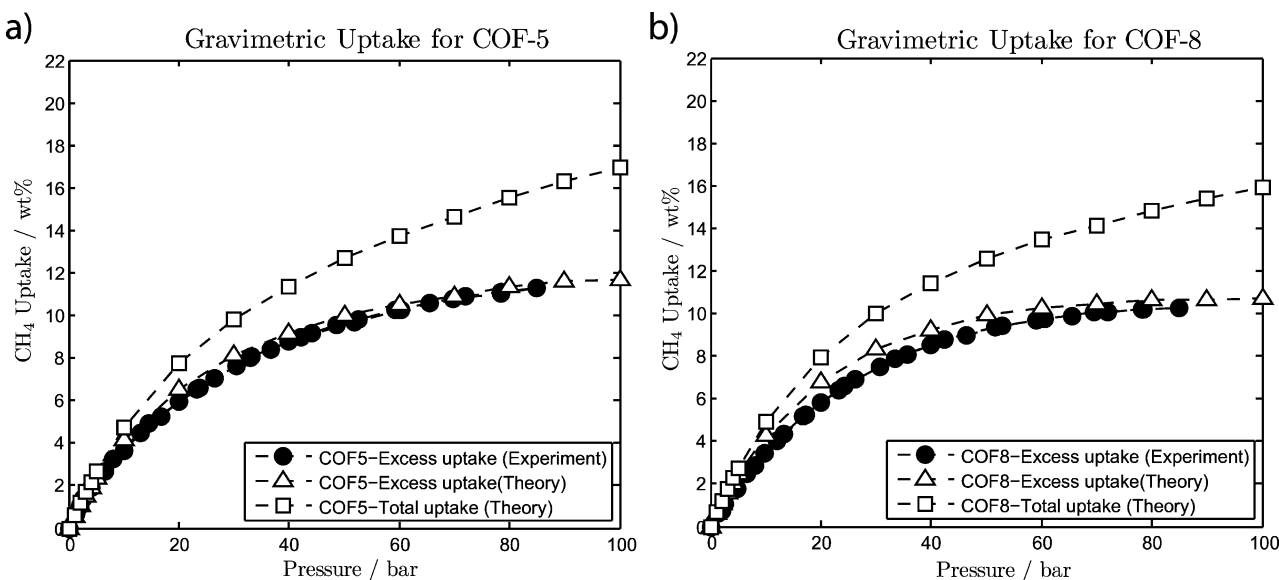
[a] r_0 is the equilibrium bond distance defined as the distance between the barycenter of every molecule.

temperatures (260−400 K) and pressures (1, 10, and 100 bar, see Supporting Information) and by comparing the sorption isotherms to our experimental results for two COFs.

2.3. GCMC Procedure. To determine methane storage capacity in COFs, we used the GCMC method with the ab initio based FF developed herein. At each step of the GCMC, one of four events (translation, rotation, creation, and annihilation of methane molecules) is applied using the Monte Carlo criteria for acceptance. Details can be found elsewhere.[31,32]

To obtain an accurate measure of methane loading, we constructed 3 000 000 configurations to compute the average loading for each thermodynamic condition. The equilibrium conditions were verified for every loading curve.

2.4. Structural Characteristics of COFs. These simulations used the experimental structures of 2D-COF (COF-1, COF-5, COF-6, COF-8, and COF-10) and 3D-COF (COF-102, COF-103, COF-105, and COF-108) shown in Figure 2. The surface area, pore volume, density, and pore aperture of studied COFs are summarized in Table 1.[33]

Figure 4. Predicted (open triangles) and experimental (closed circles) methane isotherms at 298 K in excess uptake gravimetric units (wt %): (a) COF-5; (b) COF-8. The total predicted uptake is shown by open squares.

There are two classes of 2D-COFs, one in which the layers are eclipsed and the other with them staggered.

• COF-1 has an underlying graphite topology (gra) given by the "ABAB" stacking sequence of its layers with interlayer spacing of 3.35 Å, leading to the $P6_3/mmc$ space group. This leads to compartments with pore apertures of 7 Å.[9]

• In contrast, COF-5, COF-6, COF-8, and COF-10 have a boron-nitride (bnn) topology with an "AAAA" stacking sequence of layers and $P6_3/mmm$ space group.[9,10] The pore diameters for these COFs are controlled by the building blocks (Table 1).

For the 3D-COFs, the simplest two topologies plausible from the connectivity of these building units are the carbon-nitride (ctn) and boracite (bor) topologies.[34,35]

• COF-102, COF-103, and COF-105 have the ctn topology with $I\bar{4}3d$ space group. The pore structures for these materials are similar with pore diameters varying from 12 to 19 Å.[36]

• COF-108 has the bor topology with the $P\bar{4}3m$ space group leading to two classes of pores with diameters of 11 and 20 Å.

3. Results and Discussion
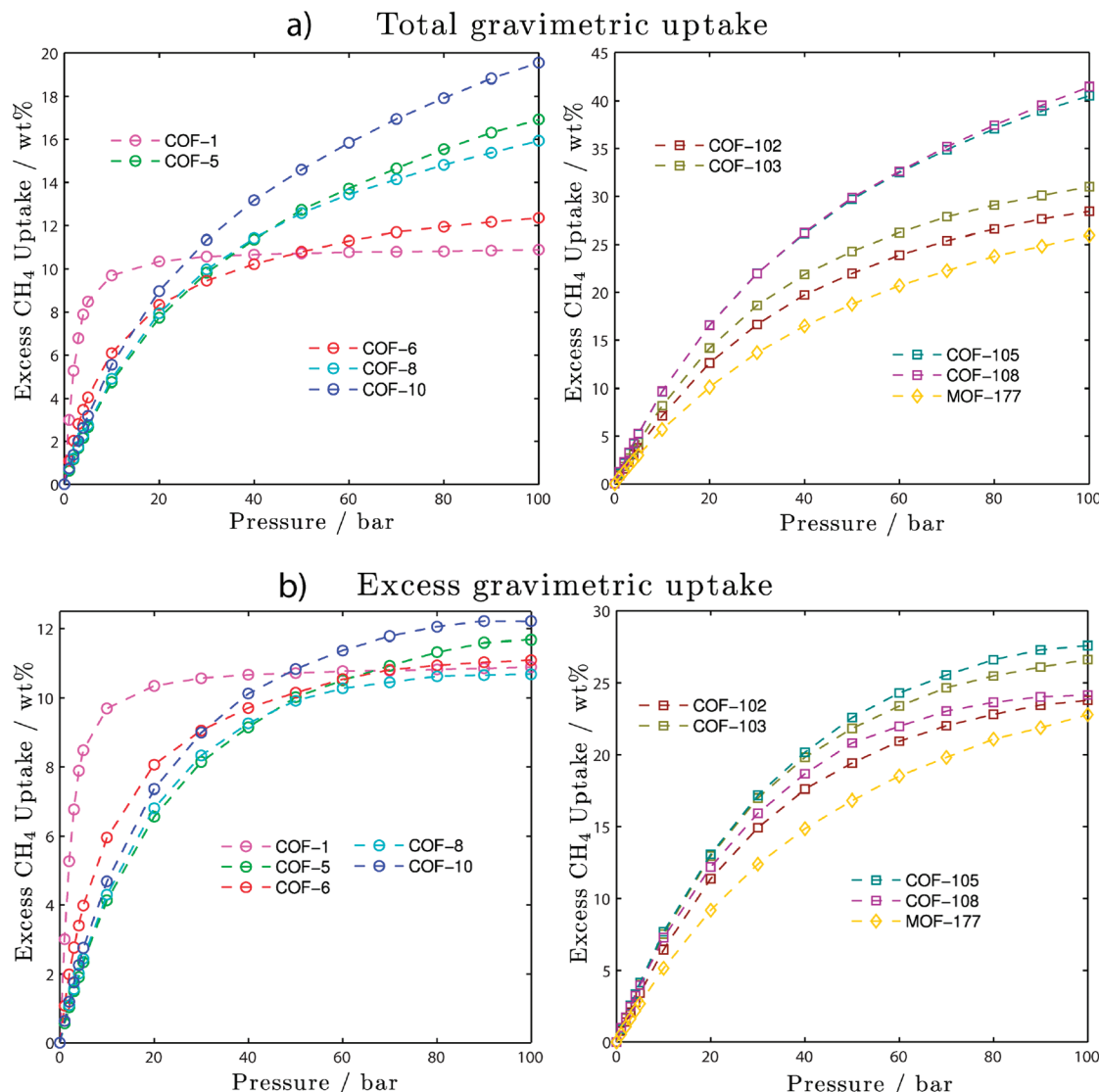
3.1. Comparison between Theoretical and Experimental Methane Adsorption Isotherms of COF-5 and COF-8. To validate our FF and simulation procedure, we additionally compare the predicted and experimental methane uptakes for COF-5 and COF-8, the two systems for which we had already confirmed to be properly activated. This was done by comparing the measured pore volume with Ar at low pressure and the measured pore volume from He at high pressure (see Supporting Information). It is very important to note that if solvent molecules remain in the pore or COF framework or are partially decomposed, it is not possible to obtain an accurate measure of the adsorption. Indeed, this is the value of the simulations, in that adsorption performance can be obtained prior to confirming proper activation. Furukawa et al.[37] reported that there are some COFs that still need to be further activated, a possible solution could the CO_2 method developed by Nelson et al.[38] The GCMC-predicted total methane adsorption isotherms for COF-5 and COF-8 at 298 K based on the new FF were converted to obtain the excess isotherms because total uptakes are not experimentally accessible.[39]

Figure 4 compares the excess isotherms in gravimetric unit (wt %) from simulations and experiments. Here wt % = (mass of gas) × 100/[(mass of framework) + (mass of the gas)]. The predicted excess methane uptake in COF-5 is 11.3 wt % at 80 bar, in excellent agreement with the experimental value of 11.1 wt % at 78 bar. Similarly, the predicted excess uptake in COF-8 of 10.6 wt % at 80 bar is very close to the experimental result of 10.3 wt % at 78 bar. These results validate our theoretical methodology for these large pore materials; indeed, COF-5 can be classified as mesoporous while COF-8 is microporous. This indicates that our FF provides a good estimation of the COF−methane interaction at 298 K. This validation of our simulation procedures allows us to determine the performance of the other COF systems, providing a guide to determine the optimal materials for methane uptake.

3.2. Gravimetric Methane Uptake in Other COFs. The predicted gravimetric methane uptakes in other COFs at 298 K are shown in Figure 5. To show superior capability of several COFs over MOFs, we have also included the experimental and theoretical methane uptake of MOF-177, which have not been reported in the literature yet. MOF-177 has been a benchmark for the MOFs compounds because of the high surface area (∼4700 m²/g)[39] and the large amount of exposed edges of the organic ligands that has been suggested to be the reason of the high permance for gas adsorption, as well as its microporosity.[40] The simulated methane adsorption isotherms of the MOF-177 are compared to the experimental data, giving a good agreement as for COFs where the combination rules have been used as well as our accurate parameters previous developed for Zn (see Supporting Information).[41] As expected, all COFs show type I for total and excess isotherms, with profiles that depend strongly on the materials. The highest *total* gravimetric methane uptake was found in COF-108 (41.5 wt %) and COF-105 (40.5 wt %), followed by COF-103 (31.0 wt %), COF-102 (28.4 wt %), MOF-177 (25.9%), COF-10 (19.6 wt %), COF-8 (15.9 wt %), COF-6 (12.3 wt %), COF-5 (16.9 wt %), and COF-1 (10.9 wt %) all at 100 bar. This is in disagreement with a recent report by Lan et al.[42] where it is shown that at 100 bar the total gravimetric uptake is 54.39% for COF-105 and 54.68% for COF-108. This is an overestimation of ∼31% with repect to our values. This might be due to the fact that only one

Methane in Covalent Organic Frameworks

J. Phys. Chem. A, Vol. 114, No. 40, 2010 **10829**

Figure 5. Predicted gravimetric methane isotherms at 298 K: (a) total and (b) excess uptake isotherms. We have also validated our calculations for MOF-177 with experiments and these are included for comparison.

configuration was used for the organic linker-CH_4 interaction and the CH_4-CH_4 parameters were not obtained with the same methodology as the other parameters.
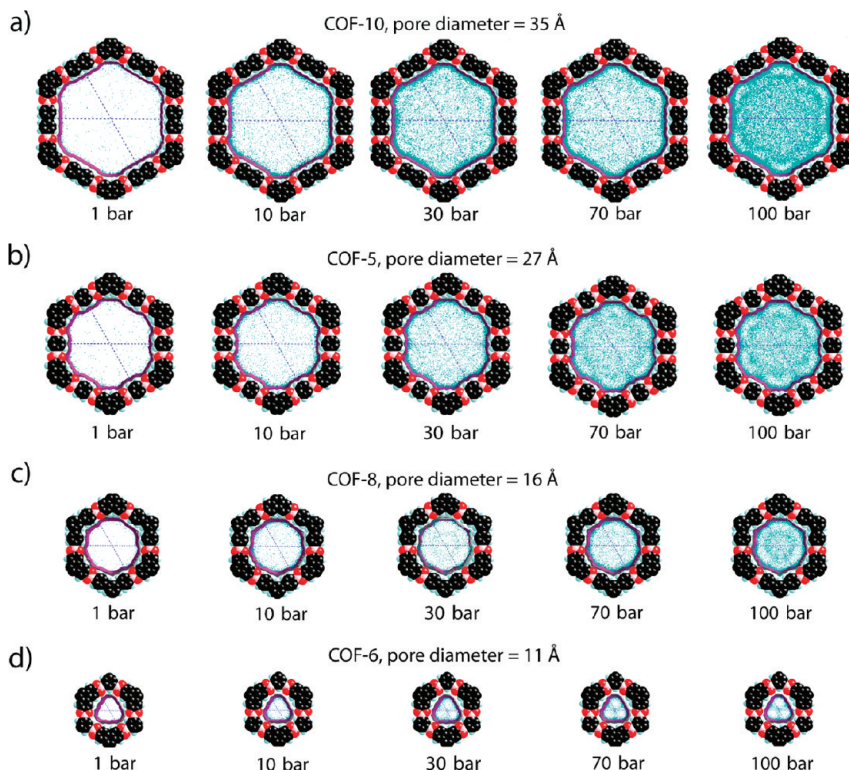
In terms of excess methane uptake (the quantity measured experimentally), the best at 100 bar are the 3D-COFs [COF-105 (27.6 wt %), COF-103 (26.6 wt %), COF-108 (24.2 wt %), and COF-102 (23.8 wt %)] followed by MOF-177 (22.8%) and 2D-COFs [COF-10 (12.2 wt %), COF-5 (11.7 wt %), COF-6 (11.1 wt %), COF-1 (10.9 wt %), and COF-8 (10.7 wt %)]. Most COFs have much smaller excess/total uptake ratios, generally in inverse proportion to the free volume (see Supporting Information): 0.81 for COF-5, 0.95 for COF-6, 0.81 for COF-8, 0.77 for COF-10, 0.89 for COF-102, 0.90 for COF-103, 0.76 for COF-105, and 0.71 for COF-108 and 0.92 for MOF-177. However, COF-1 shows an unusual behavior. It has the best performance below 30 bar, with a total uptake amount very close to the excess uptake with no additional adsorption above 30 bar. The reason is that COF-1 has parallel exposed faces of boroxine rings spaced at ~12 Å (Figure 2) and part of the benzene rings inside the pores. This leads to saturation at lower pressure and low total uptakes. The pores in COF-1 have small diameters (7 Å) and are isolated due to the "ABAB" stacking sequence; therefore, the COF-1 might have kinetically

inaccessible regions. However, the GCMC simulation assumes that any points within the simulation cell can be accessed so that our results for the case of COF-1 might overestimate the adsorption observed experimentally. This implies that the difussion rate of methane in the COF-1 pores is not very high.
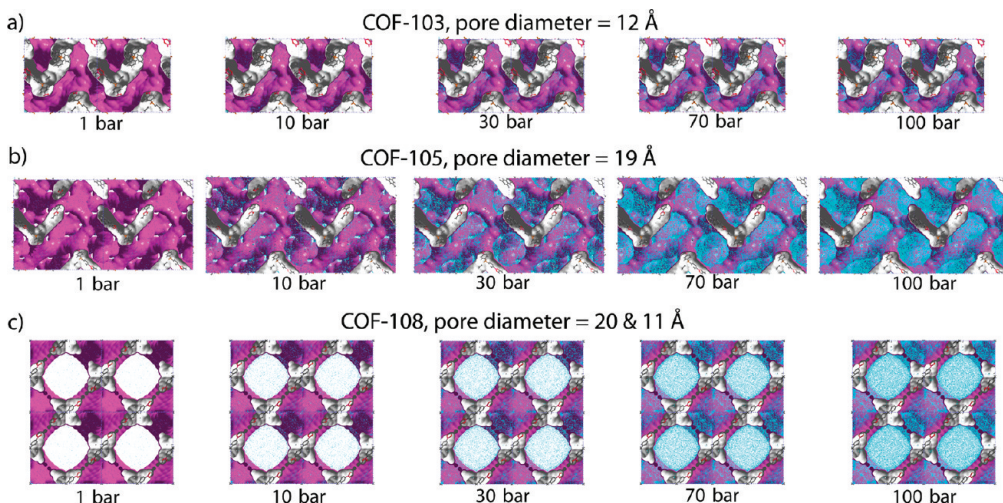
In sorption experiments, the absolute adsorbed amount can be estimated by using eq 3,[39]

$$N_{total} = N_{excess} + V_p \times \rho_{bulk} \qquad (3)$$

where N_{excess} is the excess mass, V_p is the pore volume, N_{total} is total adsorbed amount of methane, ρ_{bulk} is the bulk density of methane. Using eq 3, we recalculated the total uptake based on the experimental excess isotherms and experimental methane density (see Supporting Information). Calculated total uptakes from eq 3 are greater than simulated ones over the entire range of pressure. The error is <10% below 50 bar, but it is >20% for COF-1 at 100 bar. The reason is that the deviation is not negligible in the high-pressure region and for smaller pore COFs, since eq 3 does not compensate for the volume of adsorbed guests. Thus although eq 3 is convenient for a rough estimate of total uptake from experimental data, it can lead to an error in estimating total uptake, especially at high pressure.
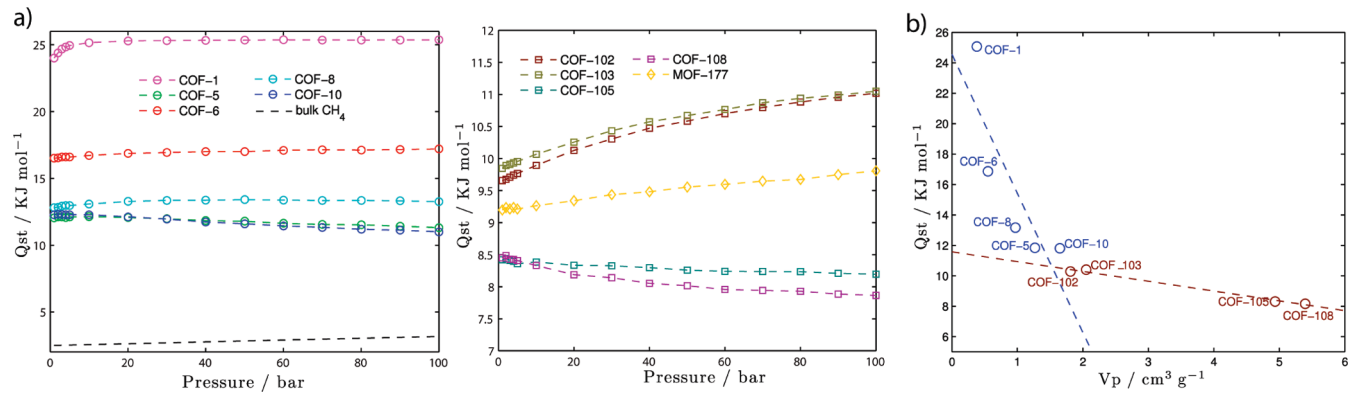
Figure 6. Ensemble average from the GCMC steps for methane adsorption in 2D-COFs at various pressures. Atom colors are the same as in Figure 2; the average of methane gas molecules are shown in blue. The accessible surface is shown in purple and was calculated using the vdw radii of every atom of the framework and the methane kinetic radii: (a) COF-10, pore diameter = 35 Å; (b) COF-5, pore diameter = 27 Å; (c) COF-8, pore diameter = 16 Å; (d) COF-6, pore diameter = 11 Å.
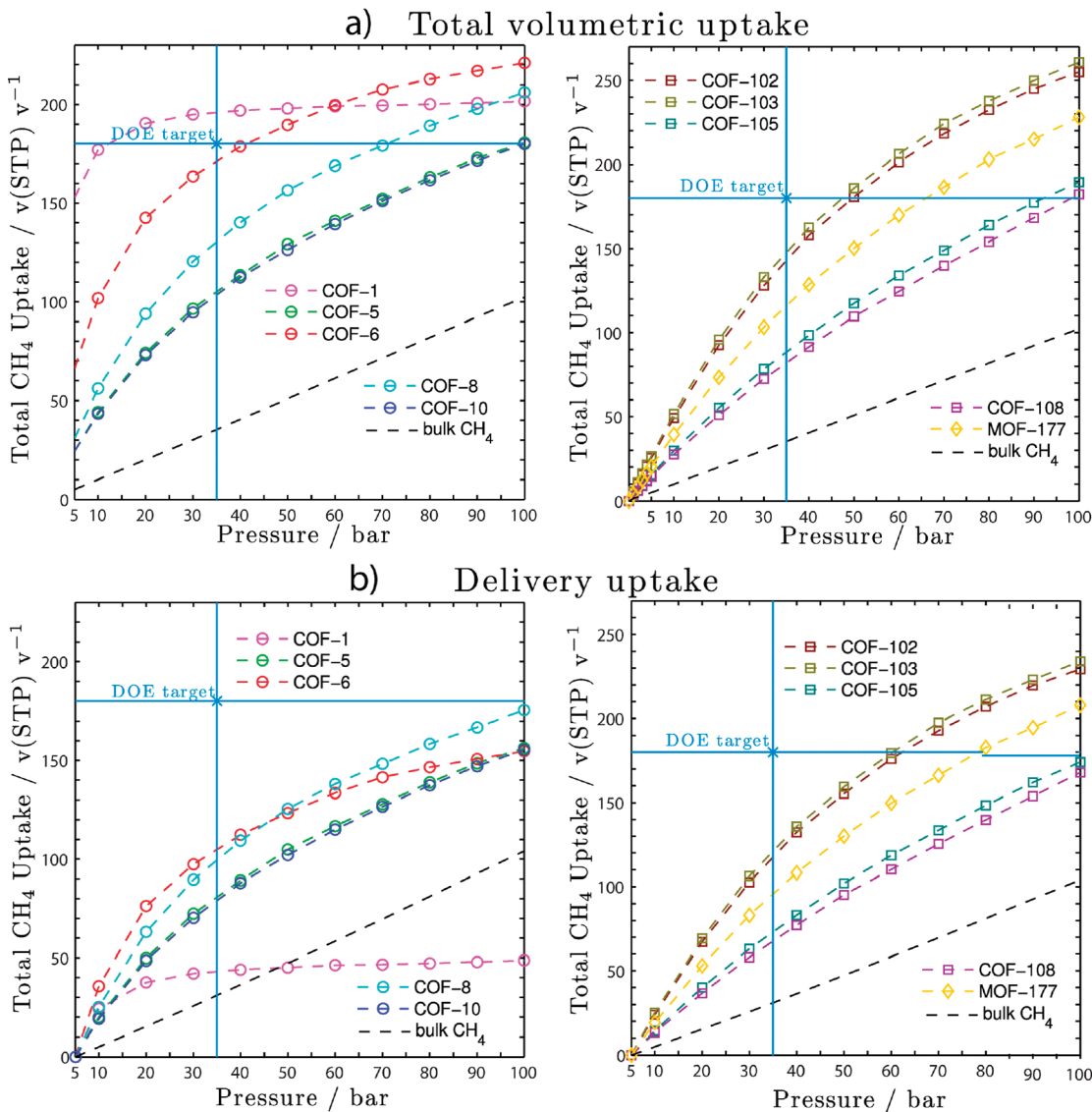
Figure 7. Ensemble average of methane molecules at different pressures: (a) COF-103; (b) COF-105; (b) COF-108. Atoms colors: C, gray; O, red; Si, yellow; B, pink. The average methane gas molecules are in blue. The accessible surface was calculated as in Figure 6. COF-102 has the same sorption profile as COF-103 and it is not shown.

3.3. Adsorption Mechanism of Methane in COFs. At cryogenic temperatures (below 20 K), entropic effects in gas adsorption are not significant, so that the specific adsorption sites of guest molecules can be observed with diffraction experiments.[43] The change in electron density is related to the strength of the adsorbent−adsorbate interaction since the electron density reflects the occupancy of the adsorption sites. However, at room temperature, such diffraction experiments do not provide clear-cut location of the guest molecules due to thermal disorder.[44] Therefore, the average of the snapshots obtained from the GCMC simulations provide new insights into the methane adsorption behavior in COFs.

Figures 6 and 7 show the average of all snapshots for every COFs under each thermodynamic condition. Figure 6 shows that the COFs with the larger pores (COF-5, 8, 10) are not filled completely even at 100 bar, although their excess isotherms show saturation, while COF-6 reaches saturation at 60 bar. Another smaller pore material, COF-1, reaches saturation at 40 bar since it can only store three methane molecules per pore (see Supporting Information). The average of the GCMC snapshots show that the joint of two edges is more populated than the center of the pore at higher pressures. Surprisingly, we find that adsorption in 2D-COFs can even occur at room temperature with the coexistence of layer formation and pore

Figure 8. (a) Predicted Q_{st} values for COFs as a function of pressure. We have added the calculated values for MOF-177 for comparison. (b) V_p versus Q_{st} for COFs. There are two groups based on the structural analysis: 2D-COFs ($-1, -5, -6, -8, -10$), which laid in a line with the same slope. Also the 3D-COFs ($-102, -103, -105, -108$) have a common line. Both lines coincide at $V_p \sim 1.53$ cm^3/g and $Q_{st} \sim 10.6$ kJ/mol.

Figure 9. Predicted volumetric methane isotherms at 298 K for COFs: (a) total uptake isotherm and (b) delivery uptake isotherm (the difference between the total amount at pressure p and that at 5 bar). Here the black dashed line indicates the uptake for free CH$_4$ gas. MOF-177 uptake is added for comparison.

filling. The formation of some patterns at higher pressures suggest the formation of a second layer for those pores that can hold them; however, a third layer is not observed even for COF-10.

Unlike 2D-COFs, the adsorption sites of 3D-COFs can be on the surface of aromatic and boroxine rings. Figure 7 shows

that the layer formation and pore filling mechanism is again present even though we are dealing with topologically different compounds. The average of the GCMC steps shows that sites that are more populated are those where two edges converge. A similar trend was observed for COF-108, although it has two different kinds of pores.

10832 *J. Phys. Chem. A, Vol. 114, No. 40, 2010*

Mendoza-Cortés et al.

3.4. Isosteric Heat of Adsorption. The adsorption enthalpy is one of the most important parameters to evaluate the performance of COFs, in addition to surface area and pore volume. We calculated the Q_{st} for COFs from their total uptake isotherms (Figure 8a). These Q_{st} values do not depend strongly on the pressure (i.e., adsorbed amounts of methane); however, we do see some interesting trends. We expect the COF−methane interaction to decrease with increasing adsorption of methane, since the stronger binding sites would be occupied first.[45] Indeed, this is the case for COF-5, COF-10, COF-105, and COF-108 (group A). However, the Q_{st} values for COF-1, COF-6, COF-8, COF-102, and COF-103 (group B) increase directly with pressure. We interpret this phenomenon as related to the pore diameters because the space is not getting wasted, this suggests that interaction of framework methane is more effective than in the bulk gas. This assumption is supported by the larger Q_{st} values of the COF−methane versus methane alone (Figure 8a). Thus group B (P_{size} below 18 Å) have an steady increase in the Q_{st} values as more methane is added to the structure, while group A (P_{size} above 18 Å) have a decrease in Q_{st} values at higher pressure; i.e., there is more space so methane can interact more, as in the bulk (see Figure 8a). MOF-177 could be classified in group B since it has a P_{size} of 10.8 Å and V_p of 1.55 cm^3/g.[40] Although it seems that the desirable pore diameter should be smaller than 18 Å, it is not always necessary to design narrow pore materials, because large Q_{st} values could have a negative impact on both heat management and diffusion rate in practical use.[46] In this sense, we believe that COF-102 and COF-103 having reasonable pore diameters and their Q_{st} values place them are among the promising materials. From the relation of Q_{st} with V_p we can find that the best materials for methane adsorption (COF-102, COF-103, and MOF-177) are found at around 1.53 cm^3/g and 10.6 kJ/mol, suggesting a maximum value of performance for these connectivities and chemical composition (Figure 8b).

3.5. Delivery Amount in COFs. In practical applications of porous material for gas storage, the delivery amount (that is, the difference in the amount adsorbed at 100 bar vs the amount, e.g., at 5 bar) is the important quantity. Although the delivery amount can be measured experimentally,[47,48] it is not easy to predict delivery amounts from excess isotherms, rather one needs total uptake isotherms. However, the simulations lead directly to this value. We choose 5 bar as the releasing pressure of cylinders and compare estimated delivery amounts to the targets set by the U.S. Department of Energy (DOE): release 180 L at standard temperature and pressure (STP), defined as 298 K and 1.01 bar, of methane per liter of storage vessel (Figure 9). The standard temperature and pressure in the DOE targets are 298 K and 1 atm. However, in the field of chemistry, one usually chooses 273 K and 1 atm as STP, so that all volumetric uptake is converted to the volume at 298 K.[49]

We see that COF-1 reaches the DOE target in a total volumetric uptake basis (195 v(STP)/v at 30 bar), but the delivery amount is very poor (42 v(STP)/v at 30 bar), making it a bad candidate for practical applications of methane storage. We predict that COF-102 and COF-103 perform very nicely in both total uptake (255 and 260 v(STP)/v at 100 bar) and delivery amount (229 and 234 v(STP)/v at 100 bar), suggesting that they are suitable for practical applications of methane storage. This results from a combination of factors such as small pore diameter, high surface area, low density, and high pore volume.

4. Concluding Remarks

To predict reliable methane adsorption isotherms, we developed FFs on the basis of accurate ab initio calculations for interactions of methane with COF subunits involving C, O, B, Si, and H. We confirmed that these calculations predict methane adsorption isotherms for COF-5 and COF-8 in good agreement with experiment. This validates that ab initio based FF can be used to obtain accurate predictions of gas adsorption isotherms. And the developed FF can be effectively used to design new materials prior to experiments.

From our GCMC trajectory, we found the multilayer formations coexist with the pore filling mechanism. We find that a pore diameter (∼12 Å), large pore volume (∼5 cm^3/g), and a high surface area (>5000 m^2/g) can lead to large volumetric methane uptakes. We also demonstrate that a high Q_{st} value can improve the initial slope for the isotherm. However, this behavior reduces the delivery amount of methane, which is more important for practical applications. There may be the misconception that a weak binding energy will necessarily result in poor methane storage capacity. However, we find that the volumetric uptake and the total uptakes in COF-102 and COF-103 outperform other 2D and 3D-COFs at high pressure, even the benchmark MOF-177. The high delivery/storage amount ratios for these COFs again support the importance of reasonable Q_{st} values. These results indicate the value of having an additional fused aromatic ring, because the methane molecules interact strongly with the faces of the aromatic or boroxine ring and weakly to the edges.

This study focused on representative crystalline COFs that have been structurally characterized. These results suggest that crystalline framework structures composed of triazines or triphosphorines instead of the boroxine rings might lead to improved properties.

Supporting Information Available: The volumetric uptake for all COFs against density, pore volume, surface area, and isosteric heat of adsorption are described. Experimental and theoretical methane uptake for MOF-177 is included. The QM energies and BSSE corrections are included. The data plotted in Figure 3 are tabulated. This material is available free of charge via the Internet at http://pubs.acs.org.

References and Notes

(1) Sun, J.; Jarvi, T. D.; Conopask, L. F.; Satyapal, S.; Rood, M. J.; Rostam-Abadi, M. *Energy Fuels* **2001**, *15*, 1241.

(2) Celzard, A.; Fierro, V. *Energy Fuels* **2005**, *19*, 573.

(3) Menon, V. C.; Komarneni, S. *J. Porous Mat.* **1998**, *5*, 43.

(4) Cracknell, R. F.; Gordon, P.; Gubbins, K. E. *J. Phys. Chem.* **1993**, *97*, 494.

(5) Fox, J. M. *Catal. Rev.-Sci. Eng.* **1993**, *35*, 169.

(6) Hickman, D. A.; Schmidt, L. D. *Science* **1993**, *259*, 343.

(7) Periana, R. A.; Taube, D. J.; Gamble, S.; Taube, H.; Satoh, T.; Fujii, H. *Science* **1998**, *280*, 560.

(8) Bhatia, S. K.; Myers, A. L. *Langmuir* **2006**, *22*, 1688.

(9) Cote, A. P.; Benin, A. I.; Ockwig, N. W.; O'Keeffe, M.; Matzger, A. J.; Yaghi, O. M. *Science* **2005**, *310*, 1166.

(10) Cote, A. P.; El-Kaderi, H. M.; Furukawa, H.; Hunt, J. R.; Yaghi, O. M. *J. Am. Chem. Soc.* **2007**, *129*, 12914.

(11) El-Kaderi, H. M.; Hunt, J. R.; Mendoza-Cortes, J. L.; Cote, A. P.; Taylor, R. E.; O'Keeffe, M.; Yaghi, O. M. *Science* **2007**, *316*, 268.

(12) Tilford, R. W.; Gemmill, W. R.; zur Loye, H. C.; Lavigne, J. J. *Chem. Mater.* **2006**, *18*, 5296.

(13) Mayo, S. L.; Olafson, B. D.; Goddard, W. A. *J. Phys. Chem.* **1990**, *94*, 8897.

Methane in Covalent Organic Frameworks

J. Phys. Chem. A, Vol. 114, No. 40, 2010 **10833**

(14) Rappe, A. K.; Casewit, C. J.; Colwell, K. S.; Goddard, W. A.; Skiff, W. M. *J. Am. Chem. Soc.* **1992**, *114*, 10024.

(15) Jorgensen, W. L.; Maxwell, D. S.; TiradoRives, J. *J. Am. Chem. Soc.* **1996**, *118*, 11225.

(16) Garberoglio, G.; Skoulidas, A. I.; Johnson, J. K. *J. Phys. Chem. B* **2005**, *109*, 13094.

(17) Garberoglio, G.; Vallauri, R. *Microporous Mesoporous Mater.* **2008**, *116*, 540.

(18) Garberoglio, G. *Langmuir* **2007**, *23*, 12154.

(19) Duren, T.; Sarkisov, L.; Yaghi, O. M.; Snurr, R. Q. *Langmuir* **2004**, *20*, 2683.

(20) Jhon, Y. H.; Cho, M.; Jeon, H. R.; Park, I.; Chang, R.; Rowsell, J. L. C.; Kim, J. *J. Phys. Chem. C* **2007**, *111*, 16618.

(21) Yang, Q. Y.; Zhong, C. L. *J. Phys. Chem. B* **2006**, *110*, 17776.

(22) Tkatchenko, A.; von Lilienfeld, O. A. *Phys. Rev. B* **2008**, *78*, 6.

(23) Waller, M. P.; Robertazzi, A.; Platts, J. A.; Hibbs, D. E.; Williams, P. A. *J. Comput. Chem.* **2006**, *27*, 491.

(24) Ahlrichs, R.; Bar, M.; Haser, M.; Horn, H.; Kolmel, C. *Chem. Phys. Lett.* **1989**, *162*, 165.

(25) Weigend, F.; Haser, M. *Theor. Chem. Acc.* **1997**, *97*, 331.

(26) Weigend, F.; Haser, M.; Patzelt, H.; Ahlrichs, R. *Chem. Phys. Lett.* **1998**, *294*, 143.

(27) Hattig, C. *Phys. Chem. Chem. Phys.* **2005**, *7*, 59.

(28) Simon, S.; Duran, M.; Dannenberg, J. J. *J. Chem. Phys.* **1996**, *105*, 11024.

(29) Rappe, A. K.; Goddard, W. A. *J. Phys. Chem.* **1991**, *95*, 3358.

(30) Pianwanit, A.; Kritayakornupong, C.; Vongachariya, A.; Selphusit, N.; Ploymeerusmee, T.; Remsungnen, T.; Nuntasri, D.; Fritzsche, S.; Hannongbua, S. *Chem. Phys.* **2008**, *349*, 77.

(31) Adams, D. J. *Mol. Phys.* **1974**, *28*, 1241.

(32) Soto, J. L.; Myers, A. L. *Mol. Phys.* **1981**, *42*, 971.

(33) Bae, Y. S.; Lee, C. H. *Carbon* **2005**, *43*, 95.

(34) Delgado-Friedrichs, O.; O'Keeffe, M.; Yaghi, O. M. *Acta Crystallogr., Sect. A* **2006**, *62*, 350.

(35) Schmid, R.; Tafipolsky, M. *J. Am. Chem. Soc.* **2008**, *130*, 12600.

(36) Yaghi, O. M.; O'Keeffe, M.; Ockwig, N. W.; Chae, H. K.; Eddaoudi, M.; Kim, J. *Nature* **2003**, *423*, 705.

(37) Furukawa, H.; Yaghi, O. M. *J. Am. Chem. Soc.* **2009**, *131*, 8875.

(38) Nelson, A. P.; Farha, O. K.; Mulfort, K. L.; Hupp, J. T. *J. Am. Chem. Soc.* **2009**, *131*, 458.

(39) Furukawa, H.; Miller, M. A.; Yaghi, O. M. *J. Mater. Chem.* **2007**, *17*, 3197.

(40) Chae, H. K.; Siberio-Perez, D. Y.; Kim, J.; Go, Y.; Eddaoudi, M.; Matzger, A. J.; O'Keeffe, M.; Yaghi, O. M. *Nature* **2004**, *427*, 523.

(41) Han, S. S.; Deng, W. Q.; Goddard, W. A. *Angew. Chem. Int. Ed.* **2007**, *46*, 6289.

(42) Lan, J. H.; Cao, D. P.; Wang, W. C. *Langmuir* **2010**, *26*, 220.

(43) Rowsell, J. L. C.; Spencer, E. C.; Eckert, J.; Howard, J. A. K.; Yaghi, O. M. *Science* **2005**, *309*, 1350.

(44) Kaszkur, Z. A.; Jones, R. H.; Waller, D.; Catlow, C. R. A.; Thomas, J. M. *J. Phys. Chem.* **1993**, *97*, 426.

(45) Llewellyn, P. L.; Maurin, G. *C. R. Chim.* **2005**, *8*, 283.

(46) Rong, Z. M.; Terzyk, A. P.; Gauden, P. A.; Vadgama, P. *J. Colloid Interface Sci.* **2007**, *313*, 449.

(47) Biloe, S.; Goetz, V.; Mauran, S. *AIChE J.* **2001**, *47*, 2819.

(48) Lozano-Castello, D.; Alcaniz-Monge, J.; de la Casa-Lillo, M. A.; Cazorla-Amoros, D.; Linares-Solano, A. *Fuel* **2002**, *81*, 1777.

(49) Burchell, T. *SAE Tech. Pap.* **2000**, *01*, 2205.